Science Advances
AAAS

advances.sciencemag.org/cgi/content/full/7/26/eabg7003/DC1

Supplementary Materials for

Nonadiabatic reaction dynamics to silicon monosulfide (SiS): A key molecular building block to sulfur-rich interstellar grains

Srinivas Doddipatla, Chao He, Shane J. Goettl, Ralf I. Kaiser*, Breno R. L. Galvão*, Tom J. Millar*

*Corresponding author. Email: ralfk@hawaii.edu (R.I.K.); brenogalvao@gmail.com (B.R.L.G.); tom.millar@qub.ac.uk (T.J.M.)

Published 25 June 2021, *Sci. Adv.* **7**, eabg7003 (2021)
DOI: 10.1126/sciadv.abg7003

This PDF file includes:

Experimental Section. The crossed molecular beam experiments of ground state silicon atoms (Si; ^3P) with deuterium sulfide (D_2S; X^1A_1) were performed in gas phase under single collision conditions exploiting a crossed molecular beam machine *(66)*. Note that the reaction was conducted with deuterium sulfide, but not with hydrogen sulfide (≥ 99 %, Sigma-Aldrich) due to the presence of traces of dihydrogendisulfide in the hydrogen sulfide lecture bottle leading to non-reactive scattering signal at the prospective products of 61 amu (HSiS) and 60 amu (SiS). This problem was overcome by using deuterium sulfide. A pulsed supersonic beam of neon-seeded ground state silicon atoms was produced via ablation of a rotating silicon rod at 266 nm (10 ± 1 mJ per pulse; 30 Hz). The ablated silicon atoms were entered into neon carrier gas (Ne; 99.999%; Specialty Gases) released from a pulsed piezoelectric valve operating at 60 Hz, a pulse width 80 μs, and a peak voltage -400 V. A four-slit chopper wheel rotating at 120 Hz selected a part of the pulsed beam defined by a peak velocity (v_p) and speed ratio (S) of 984 ± 15 m s^{-1} and 5.9 ± 0.8, respectively. Laser induced fluorescence revealed that silicon atoms are in their electronic ground state (^3P) *(78)*. This section of the beam intersected perpendicularly an early section of a pulsed beam of deuterium sulfide (97 % D; Sigma-Aldrich) characterized by a peak velocity (v_p) of 801 ± 21 ms^{-1} and a speed ratio (S) of 12.8 ± 0.8. The neutral reactive scattering products are ionized by electron impact at energy of 80 eV and 2 mA emission current; the ions are then extracted and mass filtered by a triply differentially pumped quadrupole mass filter operating in the TOF mode and detected by Daly-type ion counter; up to 2×10^5 TOF spectra were accumulated at each angle. The laboratory angular distributions were then obtained by integrating the TOF at each angle and normalized to the intensity of the TOF at the center-of-mass angle (CM). The reaction dynamics were extracted by converting the data from the laboratory frame to the CM reference frame exploiting a forward-convolution routine *(45, 46)* providing the CM translational energy $P(E_T)$ and angular $T(\theta)$ flux distribution for each channel. For barrierless reactions without threshold, a reactive cross-section with an $E_T^{-1/3}$ energy dependence; for reactions with a threshold (E_0), a $(1-E_0/E_T)$ energy dependence was utilized *(79)* . Branching ratios were calculated using the method of Krajnovich et al. *(49)* .

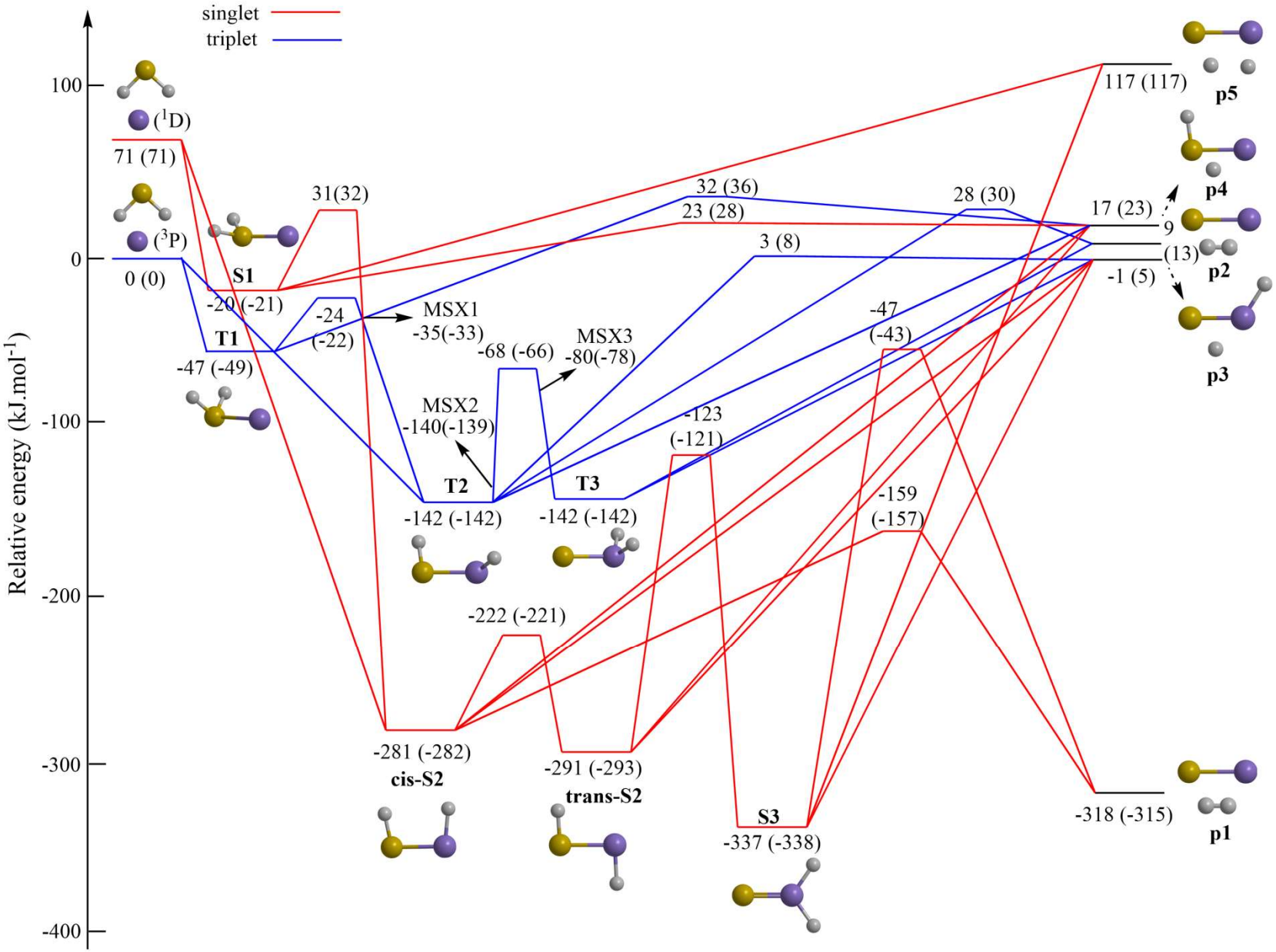
singlet
triplet
Relative energy (kJ.mol-1)
100
0
-100
-200
-300
-400
(1D)
(3P)
71 (71)
0 (0)
S1
-20 (-21)
31(32)
T1
-47 (-49)
-24
(-22)
MSX1
-35(-33)
-68 (-66)
MSX3
-80(-78)
MSX2
-140(-139)
T2
-142 (-142)
T3
-142 (-142)
-222 (-221)
-281 (-282)
cis-S2
-291 (-293)
trans-S2
S3
-337 (-338)
32 (36)
23 (28)
3 (8)
28 (30)
-123
(-121)
-47
(-43)
-159
(-157)
117 (117)
17 (23)
9
(13)
-1 (5)
-318 (-315)
p5
p4
p2
p3
p1

Fig. S1. Potential energy surface for the reactions of hydrogen sulfide (H_2S) with atomic silicon (Si) at the MRCI-F12/cc-pVQZ-F12//CASSCF/aug-cc-pV(Q+d)Z level. Relative energies are given in units of kJ mol^{-1}. Plain numbers are zero-point energies corrected for hydrogeneted reactants, whereas numbers in parentheses are for deuterated reactants. Colors of the atoms are defined as sulfur (yellow), silicon (blue), and hydrogen (gray). The cartesian coordinates and vibrational frequencies are compiled in the (Table S3).

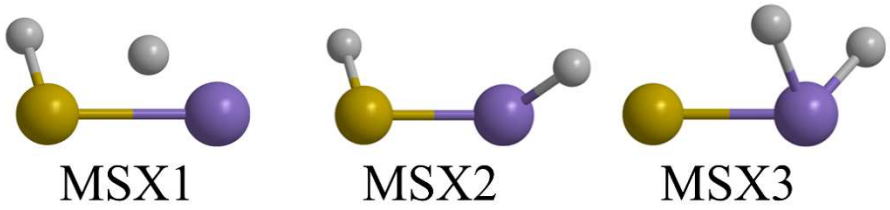

Fig. S2. Structures of minima-on-the-seam-of-crossings (MSXs).

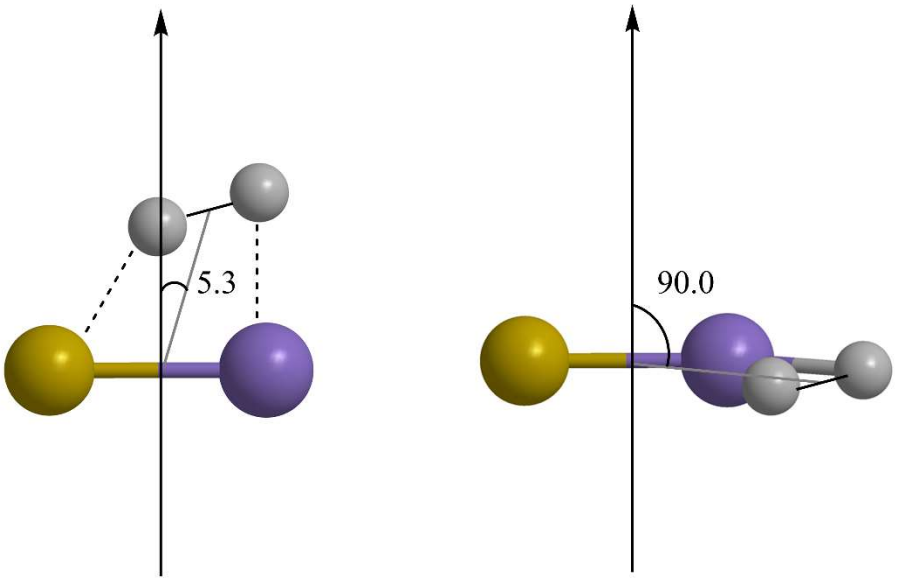

Fig. S3. Computed geometries of the exit transition states leading to the formation of SiS (p1) plus molecular deuterium from intermediates cis-**S2** (left) and **S3** (right).

Table S1. Peak velocities (v_p) and speed ratios (S) of ground state atomic silicon ($Si(^3P)$) and deuterium sulfide (D_2S; X^1A_1) beams along with the collision energy (E_C) and center-of-mass angle (Θ_{CM}).

beam	v_p (m s^{-1})	S	E_C (kJ mol^{-1})	Θ_{CM} (deg)
$Si(^3P)$	984 ± 15	5.9 ± 0.8		
D_2S (X^1A_1)	801 ± 21	12.8 ± 0.8	12.7 ± 0.4	46.3 ± 0.8

Table S2. D and D_2 loss product mass combinations of silicon and sulfur isotopes from the reaction of ground state atomic silicon and deuterium sulfide. Isotope abundance given in the parenthesis.

Si + D_2S		$D_2{}^{32}S$ (94.93%) 36	$D_2{}^{33}S$ (0.76%) 37	$D_2{}^{34}S$ (4.29%) 38
D Loss	^{28}Si (92.23%) 28	$^{28}Si^{32}SD$ 62	$^{28}Si^{33}SD$ 63	$^{28}Si^{34}SD$ 64
	^{29}Si (4.68%) 29	$^{29}Si^{32}SD$ 63	$^{29}Si^{33}SD$ 64	$^{29}Si^{34}SD$ 65
	^{30}Si (3.09%) 30	$^{30}Si^{32}SD$ 64	$^{30}Si^{33}SD$ 65	$^{30}Si^{34}SD$ 66
D_2 Loss	^{28}Si (92.23%) 28	$^{28}Si^{32}S$ 60	$^{28}Si^{33}S$ 61	$^{28}Si^{34}S$ 62
	^{29}Si (4.68%) 29	$^{29}Si^{32}S$ 61	$^{29}Si^{33}S$ 62	$^{29}Si^{34}S$ 63
	^{30}Si (3.09%) 30	$^{30}Si^{32}S$ 62	$^{30}Si^{33}S$ 63	$^{30}Si^{34}S$ 64

Table S3. Optimized Cartesian Coordinates (Å) and Vibrational Frequencies (cm^{-1}) of the reactants, products, transition states, and MSX on the singlet and triplet potential energy surfaces.

Species	Vibrational Frequencies (cm^{-1})	Cartesian Coordinates (Å)			
		Atom	X	Y	Z
H_2S 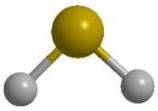	1198.66 2649.17 2673.60	S H H	0.000000 0.000000 0.000000	-0.000000 0.980451 -0.980451	-0.054937 0.873707 0.873707
T1:H_2SSi 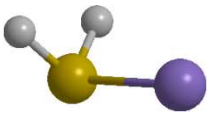	180.99 452.65 456.47 1195.18 2623.98 2642.47	S H H Si	-0.000000 0.983506 -0.983516 -0.000000	-0.057984 0.816017 0.816007 0.005839	1.143524 1.464236 1.464236 -1.415638
T2: HSSiH-T 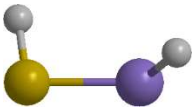	356.19 523.32 629.64 712.77 2324.36 2649.52	S H H Si	-0.017379 -1.202415 0.117356 0.058780	-0.042315 0.140549 1.276157 -0.002538	-1.003641 1.871912 -1.202526 1.121647
T3:$SSiH_2$ 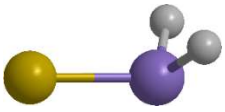	526.65 546.81 779.02 983.76 2315.08 2332.64	Si H H S	0.000013 1.215114 -1.215074 -0.000008	-0.415804 0.161026 0.161026 0.093786	1.128159 1.738861 1.738887 -0.946350
TS-diss-T1-HSSi+H 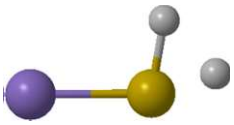	1241.64i 280.81 468.18 550.99 722.52 2553.70	S H H Si	-0.063268 -0.248702 1.496326 0.027446	-0.051584 1.264111 0.136322 0.008625	-0.956192 -1.243756 -2.112130 1.211943
TS-diss-T2-SSiH+H 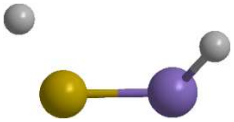	1160.07i 293.08 369.05 670.50 696.85 2245.18	S Si H H	-0.084482 0.033259 -0.057254 1.817687	0.011817 -0.058072 1.158677 0.083575	-0.923990 1.052597 1.902668 -1.842725
TS-diss-T2-SiS+H_2	1576.14i	S	-0.034198	-0.277604	-1.195345

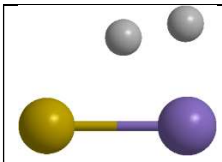	409.61 650.42 858.49 1656.42 1898.54	H H Si	0.030896 0.010530 0.003231	1.657612 1.293253 0.054909	0.666896 -0.246914 0.946863
TS-iso-T1-T2 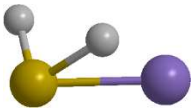	764.49i 349.98 533.83 790.94 1458.44 2594.07	S H H Si	-0.033970 -0.995963 0.574657 0.019234	-0.042377 0.645453 1.150514 -0.010937	-1.085872 0.120600 -1.292633 1.317689
TS-iso-T2-T3 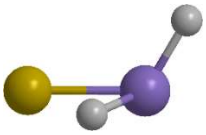	1367.75i 561.52 652.40 680.25 1713.17 2295.52	Si H H S	0.089515 1.192570 -0.798269 -0.063646	-0.429029 0.168324 0.729392 -0.018946	1.096976 1.880465 0.363414 -0.962976
S1: H_2SSi 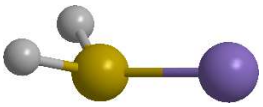	237.01 447.66 592.03 1328.08 2170.30 2378.53	S H H Si	-0.154062 0.265997 0.269769 0.052595	0.004596 -1.004536 0.997112 -0.007143	0.971997 1.797108 1.825832 -1.160358
Trans-S2: (HSSiH) 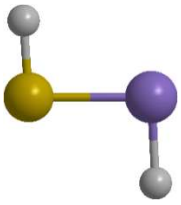	526.81 604.66 684.12 954.11 2191.62 2669.86	S H H Si	0.075031 -1.532691 1.338415 -0.115595	0.191007 -0.016944 0.639985 0.490031	-1.262024 0.873414 -1.307538 0.842247
Cis-S2: (HSSiH) 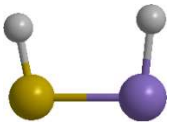	502.68 507.86 696.89 863.10 2188.78 2591.10	S H H Si	0.000005 0.000139 -0.000157 -0.000006	-0.040326 1.438803 1.284931 -0.051717	-1.004445 1.347005 -1.229789 1.142382
S3: $SSiH_2$ 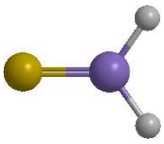	676.08 716.44 742.74 1108.26 2369.51	Si H H S	-0.000001 1.196893 -1.196846 -0.000000	-0.000001 0.000017 0.000017 0.000000	0.972899 1.826892 1.826928 -0.967161

	2375.63				
TS-diss-S1-SiSH+H 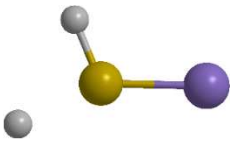	867.31i 151.61 431.08 553.68 865.07 2539.96	S H H Si	0.007998 1.178415 -0.988090 -0.015961	-0.037728 0.366882 0.421180 0.014785	0.908483 1.442400 2.484369 -1.177971
TS-diss-cisS2-SiS+H_2 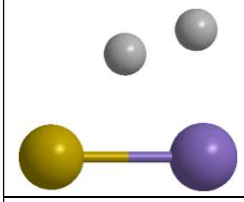	1623.18i 595.96 987.12 1012.77 1593.39 1761.39	S H H Si	-0.032598 0.031563 0.009419 0.002075	-0.232483 1.693082 1.255357 0.012213	-1.143046 0.660862 -0.273546 0.927230
TS-isom-S1-cisS2 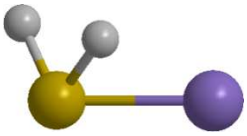	1077.46i 232.48 590.27 1275.32 1929.94 2284.54	S H H Si	0.010733 0.702898 -0.673559 -0.013305	-0.060461 0.972366 0.984744 -0.001219	1.064112 0.386708 1.651843 -1.287859
TS-isom-cisS2-transS2 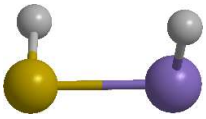	665.95i 405.95 625.92 692.29 2346.37 2539.95	S H H Si	0.249499 -1.422203 0.787729 -0.051067	-0.142744 0.642659 1.101897 0.140840	-1.332041 0.801443 -1.306465 0.896848
TS-isom-transS2-S3 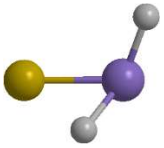	1663.18i 548.54 579.71 786.17 1784.87 2224.48	Si H H S	0.116033 1.280799 -0.940142 -0.101890	0.446121 -0.224639 -0.277625 0.027183	1.102345 0.256350 1.871131 -0.934486
TS-S3-SiS+H2 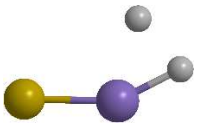	1342.25i 512.68 539.05 678.02 1143.88 2305.40	Si H H S	0.000000 0.000000 0.000000 0.000000	0.103972 -1.614781 -0.507192 -0.024369	0.984152 1.503071 2.338307 -0.982915
SiS (singlet) 	733.92	S Si	0.000000 0.000000	0.000000 0.000000	-0.908295 1.036832

SiS (triplet) 	488.72	S Si	0.000000 0.000000	0.000000 0.000000	-1.021078 1.165575
SSiH 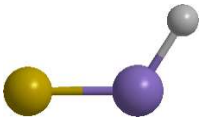	690.09 701.86 2199.56	Si S H	0.000000 0.000000 0.000000	-0.059692 0.016031 1.153351	-1.011007 0.944641 -1.875656
HSSi 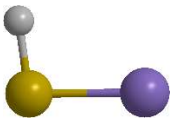	502.92 622.25 2559.67	S H Si	0.003305 -0.029846 -0.001829	0.176352 -1.129548 -0.075434	-1.019021 -1.347360 1.089941
H_2 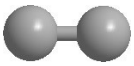	4285.17	H H	0.000000 0.000000	0.000000 0.000000	-0.377382 0.377382
MSX1 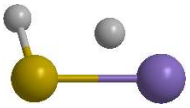	2573.91 1440.46 774.33 578.73 283.65	S H H Si	-0.005107 -1.049825 0.596803 0.022088	-0.049059 0.654129 1.146190 -0.008608	-1.084659 0.173867 -1.308290 1.278866
MSX2 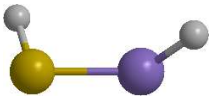	2669.15 1803.68 812.94 660.83 564.82	S H H Si	-0.013581 -1.043264 -0.043435 0.054503	-0.044940 -0.025168 1.275840 0.006416	-0.995519 2.073599 -1.229478 1.106105
MSX3 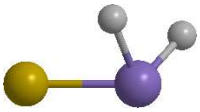	2130.73 1792.85 1072.02 754.85 277.53	Si H H S	-0.067398 0.559253 1.377742 -0.001854	-0.038147 1.010089 -0.461322 0.016165	-1.107977 -2.000754 -0.653008 1.054052

Table S4: Source data from Tercero et al*(28)*

	OHC	OPl	O15
T(K)	225	125	200
n(H_2) (cm^{-3})	5×10^7	10^6	5×10^6
Source diam (arcsec)	10	30	10
Source diam (cm)	6×10^{16}	1.8×10^{17}	6×10^{16}
N(SiS) (cm^{-2})	$(3.0 \pm 0.7) \times 10^{14}$	$(3.5 \pm 0.8) \times 10^{14}$	$(7.0 \pm 1.7) \times 10^{14}$
N(H_2) (cm^{-2})	4.2×10^{23}	2.1×10^{23}	10^{23}
f(SiS)	$(7.1 \pm 1.7) \times 10^{-10}$	$(1.7 \pm 0.4) \times 10^{-9}$	$(7.0 \pm 1.7) \times 10^{-9}$

Fractional abundances are difficult to determine for such small, dense sources because of approximations made about optical depth of observed emission lines, source size, density, and excitation temperature. As an example, the Orion Plateau source was also observed in SiS by Ziurys*(80)* in the 5-4 and 6-5 transitions with a relatively large beam, 58 and 49 arcsec, larger than the source size, 30 arcsec. In this paper she derived N(SiS) = $(2.8\text{-}3.9) \times 10^{15}$ cm^{-2} and adopted N(H_2) = 10^{24} cm^{-2} (although she noted that its value could be anywhere form $(5\text{-}50) \times 10^{23}$ cm^{-2}) to find f(SiS) = $(2.8\text{-}3.9) \times 10^{-9}$. In this analysis she adopted a rotational temperature of 230K, higher than that currently thought (125K). Ziurys *(81)*reobserved these two transitions with a different telescope and added the 15-14 transition to them. In this paper, she used a rotational temperature of 100K and derived N(SiS) = 4×10^{15} cm^{-2} for a 10 arcsec source and 1.4×10^{14} cm^{-2} for a 27 arcsec source, closer to the actual size of the plateau.

Table S5: Initial fractional abundances, f(X), of species relative to H_2

Species	Abundance	Species	Abundance
He	1×10^{-1}	CH_3OH	1×10^{-6}
H_2O	2×10^{-4}	N_2	4×10^{-7}
CO	1×10^{-4}	SiH_4	2×10^{-7}
NH_3	2×10^{-5}	OCS	1×10^{-7}
H_2S	2×10^{-6}	CH_4	1×10^{-7}

REFERENCES AND NOTES

1. A. Sarangi, M. Matsuura, E. R. Micelotta, Dust in supernovae and supernova remnants I: Formation scenarios. *Space Sci. Rev.* **214**, 63 (2018).

2. G. C. Sloan, M. Matsuura, A. A. Zijlstra, E. Lagadec, M. A. T. Groenewegen, P. R. Wood, C. Szyszka, J. Bernard-Salas, J. T. van Loon, Dust formation in a galaxy with primitive abundances. *Science* **323**, 353–355 (2009).

3. B. T. Draine, Interstellar dust grains. *Annu. Rev. Astron. Astrophys.* **41**, 241–289 (2003).

4. D. A. Williams, Gas and dust in the interstellar medium. *J. Phys. Conf. Ser.* **6**, 1–17 (2005).

5. T. Henning, Cosmic silicates. *Annu. Rev. Astron. Astrophys.* **48**, 21–46 (2010).

6. A. G. G. M. Tielens, *Nature's Nanostructures*, A. S. Barnard, H. Guo, Eds. (Pan Stanford Publishing Pte. Ltd., 2012).

7. L. M. Ziurys, The chemistry in circumstellar envelopes of evolved stars: Following the origin of the elements to the origin of life. *Proc. Natl. Acad. Sci. U.S.A.* **103**, 12274–12279 (2006).

8. A. P. Jones, J. A. Nuth-III, Dust destruction in the ISM: A re-evaluation of dust lifetimes. *Astron. Astrophys* **530**, 12 (2011).

9. S. Zhukovska, C. Dobbs, E. B. Jenkins, R. S. Klessen, Modeling dust evolution in galaxies with a multiphase, inhomogeneous ISM. *Astrophys. J.* **831**, 147 (2016).

10. M. J. Michałowski, Dust production 680–850 million years after the Big Bang. *Astron. Astrophys.* **577**, A80 (2015).

11. R. McKinnon, P. Torrey, M. Vogelsberger, Dust formation in Milky Way-like galaxies. *Mon. Not. R. Astron. Soc.* **457**, 3775–3800 (2016).

12. T. Danilovich, E. D. Beck, J. H. Black, H. Olofsson, K. Justtanont, Sulphur molecules in the circumstellar envelopes of M-type AGB stars. *Astron. Astrophys.* **588**, 24 (2016).

13. L. Podio, C. Codella, B. Lefloch, N. Balucani, C. Ceccarelli, R. Bachiller, M. Benedettini, J. Cernicharo, N. Faginas-Lago, F. Fontani, A. Gusdorf, M. Rosi, Silicon-bearing molecules in the shock L1157-B1: First detection of SiS around a Sun-like protostar. *Mon. Not. R. Astron. Soc* **470**, L16-L20 (2017).

14. A. G. G. M. Tielens, Interstellar depletions and the life cycle of interstellar dust. *Astrophys. J.* **499**, 267–272 (1998).

15. A. P. Jones, Interstellar and circumstellar grain formation and survival. *Phil. Trans. R. Soc. Lond. A* **359**, 1961–1972 (2001).

16. E. Dwek, Iron: A key element for understanding the origin and evolution of interstellar dust. *Astrophys. J.* **825**, 136 (2016).

17. H.-P. Gail, E. Sedlmayr, Mineral formation in stellar winds. I. Condensation sequence of silicate and iron grains in stationary oxygen rich outflows. *Astron. Astrophys.* **347**, 594–616 (1999).

18. A. C. Reber, S. Paranthaman, P. A. Clayborne, S. N. Khanna, A. W. Castleman Jr, From SiO molecules to silicates in circumstellar space: Atomic structures, growth patterns, and optical signatures of Si_nO_m clusters. *ACS Nano* **2**, 1729–1737 (2008).

19. D. Gobrecht, I.Cherchneff, A.Sarangi, J. M. C. Plane, S. T. Bromley, Dust formation in the oxygen-rich AGB star IK Tauri. *Astron. Astrophys.* **585**, A6 (2016).

20. H.-P. Gail, M. Scholz, A. Pucci, Silicate condensation in Mira variables. *Aastron. Astrophys.* **591**, A17 (2016).

21. M. Förstel, A. Bergantini, P. Maksyutenko, S. Góbi, R. I. Kaiser, Formation of methylamine and ethylamine in extraterrestrial ices and their role as fundamental building blocks of proteinogenic α-amino acids. *Astrophys. J.* **845**, 83 (2017).

22. D. S. N. Parker, F. Zhang, Y. S. Kim, R. I. Kaiser, A. Landera, V. V. Kislov, A. M. Mebel, A. G. G. M. Tielens, Low temperature formation of naphthalene and its role in the synthesis of PAHs

(polycyclic aromatic hydrocarbons) in the interstellar medium. *Proc. Natl. Acad. Sci. U.S.A.* **109**, 53–58 (2012).

23. S. A. Krasnokutski, G. Rouillé, C. Jäger, F. Huisken, S. Zhukovska, T. Henning, Formation of silicon oxide grains at low temperature. *Astrophys. J.* **782**, 15 (2014).

24. T. Yang, A. M. Thomas, B. B. Dangi, R. I. Kaiser, A. M. Mebel, T. J. Millar, Directed gas phase formation of silicon dioxide and implications for the formation of interstellar silicates. *Nat. Commun.* **9**, 774 (2018).

25. L. V. Prieto, C. S. Contreras, J. Cernicharo, M. Agúndez, G. Quintana-Lacaci, V. Bujarrabal, J. Alcolea, C. Balança, F. Herpin, K. M. Menten, F. Wyrowski, The millimeter IRAM-30 m line survey toward IK Tauri. *Astron. Astrophys.* **597**, A25 (2017).

26. L. Decin, A. M. S. Richards, T. Danilovich, W. Homan, J. A. Nuth, ALMA spectral line and imaging survey of a low and a high mass-loss rate AGB star between 335 and 362 GHz. *Astron. Astrophys.* **615**, A28 (2018).

27. F. L. Schöier, J. Bast, H. Olofsson, M. Lindqvist, The abundance of SiS in circumstellar envelopes around AGB stars. *Astron. Astrophys.* **473**, 871–882 (2007).

28. B. Tercero, L. Vincent, J. Cernicharo, S. Viti, N. Marcelino, A line-confusion limited millimeter survey of Orion KL. II. Silicon-bearing species. *Astron. Astrophys.* **528**, A26 (2011).

29. D. F. Dickinson, E. N. R. Kuiper, Interstellar silicon sulfide. *Astrophys. J.* **247**, 112–115 (1981).

30. I. Cherchneff, A chemical study of the inner winds of asymptotic giant branch stars. *Astron. Astrophys.* **456**, 1001–1012 (2006).

31. S. Massalkhi, M. Agúndez, J. Cernicharo, Study of CS, SiO, and SiS abundances in carbon star envelopes: Assessing their role as gas-phase precursors of dust. *Astron. Astrophys.* **628**, A62 (2019).

32. S. Zhukovska, H.-P. Gail, Condensation of MgS in outflows from carbon stars. *Astron. Astrophys.* **486**, 229–237 (2008).

33. K. Smolders, P. Neyskens, J. A. D. L. Blommaert, S. Hony, H. van Winckel, L. Decin, S. V. Eck, G. C. Sloan, J. Cami, S. Uttenthaler, P. Degroote, D. Barry, M. Feast, M. A. T. Groenewegen, M. Matsuura, J. Menzies, R. Sahai, J. T. van Loon, A. A. Zijlstra, B. Acke, S. Bloemen, N. Cox, P. De Cat, M. Desmet, K. Exter, D. Ladjal, R. Østensen, S. Saesen, F. vanWyk, T. Verhoelst, W. Zima, The Spitzer spectroscopic survey of S-type stars. *Astron. Astrophys* **540**, A72 (2012).

34. P. Hoppe, K. Lodders, W. Fujiya, Sulfur in presolar silicon carbide grains from asymptotic giant branch stars. *Meteorit. Planet. Sci.* **50**, 1122–1138 (2015).

35. D. McElroy, C. Walsh, A. J. Markwick, M. A. Cordiner, K. Smith, T. J. Millar, The UMIST database for astrochemistry 2012. *Astron. Astrophys.* **550**, A36 (2013).

36. C. M. Andreazza, E. P. Marinho, Silicon monosulphide radiative association. *Mon. Not. R. Astron. Soc.* **380**, 365–368 (2007).

37. M. A. M. Paiva, B. Lefloch, B. R. L. Galvão, SiS formation via gas phase reactions between atomic silicon and sulphur-bearing species. *Mon. Not. R. Astron. Soc.* **493**, 299–304 (2020).

38. A. Zanchet, O. Roncero, M. Agúndez, J. Cernicharo, Formation and Destruction of SiS in Space. *Astrophys. J.* **862**, 38 (2018).

39. M. Rosi, L. Mancini, D. Skouteris, C. Ceccarelli, N. F. Lago, L. Podio, C. Codella, B. Lefloch, N. Balucani, Possible scenarios for SiS formation in the interstellar medium: Electronic structure calculations of the potential energy surfaces for the reactions of the SiH radical with atomic sulphur and S_2. *Chem. Phys. Lett.* **695**, 87–93 (2018).

40. T. Glenewinkel-Meyer, J. A. Bartz, G. M. Thorson, F. F. Crim, The vacuum ultraviolet photodissociation of silane at 125.1 nm. *J. Chem. Phys.* **99**, 5944–5950 (1993).

41. M. Suto, L. C. Lee, Quantitative photoexcitation study of SiH_4 in vacuum ultraviolet. *J. Chem. Phys.* **84**, 1160–1164 (1986).

42. J. Holdship, S. Viti, I. Jimenez-Serra, B. Lefloch, C. Codella, L. Podio, M. Benedettini, F. Fontani, R. Bachiller, M. Tafalla, C. Ceccarelli, H_2S in the L1157-B1 bow shock. *Mon. Not. R. Astron. Soc.* **463**, 802–810 (2016).

43. T. Danilovich, M. V. d Sande, E. D. Beck, L. Decin, H. Olofsson, S. Ramstedt, T. J. Millar, Sulphur-bearing molecules in AGB stars. I. The occurrence of hydrogen sulphide. *Astron. Astrophys.* **606**, A124 (2017).

44. R. D. Levine, R. B. Bernstein, *Molecular Reaction Dynamics and Chemical Reactivity* (Oxford Univ. Press, 1987), pp. 26–86.

45. M. F. Vernon, Thesis, University of California, Berkeley, USA (1983).

46. P. S. Weiss, Thesis, University of California, Berkeley, USA (1986).

47. R. D. Levine, *Molecular Reaction Dynamics* (Cambridge Univ. Press, 2005).

48. W. B. Miller, S. A. Safronan, D. R. Herschbach, Exchange reactions of alkali atoms with alkali halides: A collision complex mechanism. *Discuss. Faraday Soc.* **44**, 108–122 (1967).

49. D. Krajnovich, F. Huisken, Z. Zhang, Y. R. Shen, Y. T. Lee, Competition between atomic and molecular chlorine elimination in the infrared multiphoton dissociation of CF_2CI_2. *J. Chem. Phys.* **77**, 5977–5989 (1982).

50. H.-J. Werner, P. J. Knowles, A second order multiconfiguration SCF procedure with optimum convergence. *J. Chem. Phys.* **82**, 5053–5063 (1985).

51. P. J. Knowles, H.-J. Werner, An efficient second-order MC SCF method for long configuration expansions. *Chem. Phys. Lett.* **115**, 259–267 (1985).

52. T. H. Dunning Jr, K. A. Peterson, A. K. Wilson, Gaussian basis sets for use in correlated molecular calculations. X. The atoms aluminum through argon revisited. *J. Chem. Phys.* **114**, 9244–9253 (2001).

53. T. Shiozaki, G. Knizia, H.-J. Wernera, Explicitly correlated multireference configuration interaction: MRCI-F12. *J. Chem. Phys.* **134**, 034113 (2011).

54. T. Shiozaki, H.-J. Wernera, Explicitly correlated multireference configuration interaction with multiple reference functions: Avoided crossings and conical intersections. *J. Chem. Phys.* **134**, 184104 (2011).

55. T. Shiozaki, H.-J. Werner, Topical review: Multireference explicitly correlated F12 theories. *Mol. Phys.* **111**, 607–630 (2013).

56. K. A. Peterson, T. B. Adler, H.-J. Werner, Systematically convergent basis sets for explicitly correlated wavefunctions: The atoms H, He, B–Ne, and Al–Ar. *J. Chem. Phys.* **128**, 084102 (2008).

57. I. Pérez-Justea, L. Carballeira, Theoretical study of the electronic structure of HXY/XYH radicals (X=C,Si; Y=O,S). *J. Chem. Phys.* **127**, 164303 (2007).

58. P. J. Bruna, F. Grein, Theoretical investigation of the structures and relative energies of the isomer pairs HSiS/SiSH, $HSiS^+/SiSH^+$, and $HSiS^-/SiSH^-$. *J. Phys. Chem.* **96**, 6617–6623 (1992).

59. X. Liu, X. Liu, X. Wang, Splitting of hydrogen sulfide by group 14 elements (Si, Ge, Sn, Pb) in excess argon at cryogenic temperatures. *J. Phys. Chem. A* **122**, 7023–7032 (2018).

60. C.-H. Lai, M.-D. Su, S.-Y. Chu, Structures, vibrational spectra, and relative energies of HXSiS (X = H, F, and Cl) isomers. *Int. J. Quant. Chem.* **82**, 14–25 (2001).

61. T. Kudo, S. Nagase, Theoretical study of silanethione ($H_2Si=S$) in the ground, excited, and protonated states: Comparison with silanone ($H_2Si=O$). *Organometallics* **5**, 1207–1215 (1986).

62. T. H. G. Vidal, V. Wakelam, A new look at sulphur chemistry in hot cores and corinos. *Mon. Not. R. Astron. Soc.* **474**, 5575–5587 (2018).

63. P. A. Cook, S. R. Langford, R. N. Dixon, M. N. R. Ashfold, An experimental and ab initio reinvestigation of the Lyman-α photodissociation of H_2S and D_2S. *J. Chem. Phys.* **114**, 1672–1684 (2001).

64. D. E. Woon, E. Herbst, Quantum chemical predictions of the properties of known and postulated neutral interstellar molecules. *Astrophys. J. Suppl. Ser.* **185**, 273–288 (2009).

65. F. X. Brown, S. Yamamoto, S. Saito, The microwave spectrum of the HSiS radical in the ^{2}A′ ground electronic state. *J. Mol. Struct.* **413**, 537–544 (1997).

66. T. Yang, L. Bertels, B. B. Dangi, X. Lid, M. Head-Gordon, R. I. Kaiser, Gas phase formation of c-SiC_3 molecules in the circumstellar envelope of carbon stars. *Proc. Natl. Acad. Sci. U.S.A.* **116**, 14471–14478 (2019).

67. H.-J. Werner, P. J. Knowles, G. Knizia, F. R. Manby, M. Schütz, P. Celani, W. Györffy, D. Kats, T. Korona, R. Lindh, A. Mitrushenkov, G. Rauhut, K. R. Shamasundar, T. B. Adler, R. D. Amos, A. Bernhardsson, A. Berning, D. L. Cooper, M. J. O. Deegan, A. J. Dobbyn, F. Eckert, E. Goll, C. Hampel, A. Hesselmann, G. Hetzer, T. Hrenar, G. Jansen, C. Köppl, Y. Liu, A. W. Lloyd, R. A. Mata, A. J. May, S. J. McNicholas, W. Meyer, M. E. Mura, A. Nicklass, D. P. O'Neill, P. Palmieri, D. Peng, K. Pflüger, R. Pitzer, M. Reiher, T. Shiozaki, H. Stoll, A. J. Stone, R. Tarroni, T. Thorsteinsson, M. Wang, Version 2015.1, A package of ab initio programs (2015), vol. MOLPROSS.

68. T. Trabelsi, J. S. Francisco, Is AlOH the astrochemical reservoir molecule of AlO?: Insights from excited electronic states. *Astrophys. J* **863**, 139 (2018).

69. H.-J. Werner, P. J. Knowles, An efficient internally contracted multiconfiguration-reference configuration interaction method. *J. Chem. Phys.* **89**, 5803–5814 (1988).

70. P. J. Knowles, H.-J. Werner, An efficient method for the evaluation of coupling coefficients in configuration interaction calculations. *Chem. Phys. Lett.* **145**, 514–522 (1988).

71. A. Berning, M. Schweizer, H.-J. Werner, P. J. Knowles, P. Palmieri, Spin-orbit matrix elements for internally contracted multireference configuration interaction wavefunctions. *Mol. Phys.* **98**, 1823–1833 (2000).

72. N. Koga, K. Morokuma, Determination of the lowest energy point on the crossing seam between two potential surfaces using the energy gradient. *Chem. Phys. Lett.* **119**, 371–374 (1985).

73. J. N. Harvey, M. Aschi, Spin-forbidden dehydrogenation of methoxy cation: A statistical view. *Phys. Chem. Chem. Phys.* **1**, 5555–5563 (1999).

74. K. L. Gannon, M. A. Blitz, C.-H. Liang, M. J. Pilling, P. W. Seakins, D. R. Glowacki, J. N. Harvey, An experimental and theoretical investigation of the competition between chemical reaction and relaxation for the reactions of $^1CH_2$ with acetylene and ethene: Implications for the chemistry of the giant planets. *Faraday Discuss.* **147**, 173–188 (2010).

75. B. Tercero, J. Cernicharo, J. R. Pardo, J. R. Goicoechea, A line confusion limited millimeter survey of Orion KL. I. Sulfur carbon chains. *Astron. Astrophys* **517**, A96 (2010).

76. S. Doddipatla, C. He, R. I. Kaiser, Y. Luo, R. Sun, G. R. Galimova, A. M. Mebel, T. J. Millar, A chemical dynamics study on the gas phase formation of thioformaldehyde (H_2CS) and its thiohydroxycarbene isomer (HCSH). *Proc. Natl. Acad. Sci. U.S.A.* **117**, 22712–22719 (2020).

77. N. R. Crockett, E. A. Bergin, J. L. Neill, J. H. Black, G. A. Blake, M. Kleshcheva, Herschel observations of extra-ordinary sources: H_2S as a probe of dense gas and possibly hidden luminosity toward the Orion KL hot core. *Astrophys. J.* **781**, 114 (2014).

78. T. Yang, B. B. Dangi, R. I. Kaiser, K.-H. Chao, B.-J. Sun, A. H. H. Chang, T. L. Nguyen, J. F. Stanton, Gas-phase formation of the disilavinylidene (H_2SiSi) transient. *Angew. Chem. Int. Ed.* **56**, 1264–1268 (2017).

79. R. D. Levine, *Molecular Reaction Dynamics and Chemical Reactivity* (Oxford Univ. Press, 1989).

80. L. M. Ziurys, SiS in Orion-KL: Evidence for "outflow" chemistry. *Astrophys. J.* **324**, 544–552 (1988).

81. L. M. Ziurys, SiS in outflow regions: More high-temperature silicon chemistry. *Astrophys. J.* **379**, 260–266 (1991).